



January 2014

Tribology Of Novel Multifunctional MAX Phase Composites

Ryan Roy Johnson

Follow this and additional works at: <https://commons.und.edu/theses>

Recommended Citation

Johnson, Ryan Roy, "Tribology Of Novel Multifunctional MAX Phase Composites" (2014). *Theses and Dissertations*. 1668.
<https://commons.und.edu/theses/1668>

This Thesis is brought to you for free and open access by the Theses, Dissertations, and Senior Projects at UND Scholarly Commons. It has been accepted for inclusion in Theses and Dissertations by an authorized administrator of UND Scholarly Commons. For more information, please contact zeinebyousif@library.und.edu.

TRIBOLOGY OF NOVEL MULTIFUNCTIONAL MAX PHASE
COMPOSITES

by

Ryan Roy Johnson

Bachelor of Science, University of North Dakota, 2013

A Thesis
Submitted to the Graduate Faculty
of the
University of North Dakota
In partial fulfillment of the requirements
for the degree of
Master of Science

Grand Forks, North Dakota

December

2014

Copyright 2014 Ryan R. Johnson

This thesis, submitted by Ryan Roy Johnson in partial fulfillment of the requirements for the Degree of Master of Sciences in Mechanical Engineering from the University of North Dakota, has been read by the Faculty Advisory Committee under whom the work has been done and is hereby approved.

Surojit Gupta, Ph.D.

Matthew Cavalli, Ph.D., P.E.

Bishu Bandyopadhyay, PhD.

This thesis is being submitted by the appointed advisory committee as having met all of the requirements of the Graduate School at the University of North Dakota and is hereby approved.

Wayne Swisher, Ph.D

Date

PERMISSION

Title Tribology of Novel Multifunctional MAX Phase Composites
Department Mechanical Engineering
Degree Master of Science

In presenting this thesis in partial fulfillment of the requirements for a graduate degree from the University of North Dakota, I agree that the library of this University shall make it freely available for inspection. I further agree that permission for extensive copying for scholarly purposes may be granted by the professor who supervised my thesis work or, in his absence, by the Chairperson of the department or the Dean of the Graduate School. It is understood that any copying or publication or other use of this thesis or part thereof for financial gain shall not be allowed without my written permission. It is also understood that due recognition shall be given to me and the University of North Dakota in any scholarly use which may be made of any material in my thesis.

Ryan Roy Johnson

December 04, 2014

TABLE OF CONTENTS

ACKNOWLEDGMENTS	ix
ABSTRACT.....	x
CHAPTER	
I. ALUMINUM / MAX PHASE (MAXMET) TRIBOLOGY	1
INTRODUCTION	1
METHODS	3
DATA AND ANALYSIS	5
<i>1.1 Tribological Behavior</i>	5
<i>1.2 Investigation of Tribosurfaces</i>	10
<i>1.3 Mechanisms</i>	11
CONCLUSIONS.....	12
II. TIN / MAX PHASE (MAXMET) TRIBOLOGY	13
INTRODUCTION	13
METHODS	14
DATA AND ANALYSIS	16
<i>2.1 Tribological Behavior</i>	16
<i>2.2 Investigation of Tribosurfaces</i>	18
CONCLUSIONS.....	20

III.	EPOXY / MAX PHASE (MAXPOL).....	21
	INTRODUCTION	21
	METHODS	22
	DATA AND ANALYSIS	24
	3.1 Tribological Behavior.....	24
	3.3 Investigation of Tribosurfaces	30
	3.4 Fundamental Mechanisms	34
	CONCLUSIONS.....	36
IV.	FUTURE WORK.....	37
	APPENDICES	40
	STATUS OF JOURNAL PUBLICATIONS.....	40
	CONTRIBUTED PRESENTATIONS	40
	REFERENCES	43
	CHAPTER I	43
	CHAPTER II	46
	CHAPTER III	47
	CHAPTER IV	51

LIST OF FIGURES

FIGURE	PAGE
1. Figure 1: Tribological behavior of, (a) Al, (b) Al(95)-Ti ₃ SiC ₂ (5), (c) Al(90)-Ti ₃ SiC ₂ (10), (d) Al(80)-Ti ₃ SiC ₂ (20), and (e) Al(65)-Ti ₃ SiC ₂ (35) against alumina	7
2. Figure 2: Summary of, (a) Final friction coefficient (μ_f) and (b) Wear Rate (WR).	9
3. Figure 3: SEM micrographs of, (a) Al(80)-Ti ₃ SiC ₂ (20) low, and (b) Al(80)-Ti ₃ SiC ₂ (20) high magnification, and (c) Al ₂ O ₃ surface.	11
4. Figure 4: Plot of, (a) Coefficient of friction and Wear Rate Versus Vol% of Ti ₃ SiC ₂ additions in a Sn matrix, and (b) Coefficient of Friction versus distance of Sn(70)-Ti ₃ SiC ₂ (30) and Sn samples against alumina.	17
5. Figure 5: SE SEM micographs of, (a) Al ₂ O ₃ Substrate (low magnification), and (b) Al ₂ O ₃ Substrate (high magnification), (c) Sn(70)-Ti ₃ SiC ₂ (30) and, (d) BSE image of the same surface.....	19
6. Figure 6: Tribological behavior of Epoxy-Ti ₃ SiC ₂ against, (a) Inconel 718 (first 200 m), (b) Inconel 718, (c) alumina (first 200 m), and (d) alumina..	26
7. Figure 7: Change in μ as a function of sliding distance when Ti ₃ SiC ₂ was tested against Inconel 718 [25].	27
8. Figure 8: Summary of tribological behavior of Ti ₃ SiC ₂ -epoxy composites against, (a) Inconel 718, and (b) alumina substrates.....	28

9. Figure 9: SE SEM micrographs of, (a) Substrate (lower magnification), (b) Substrate (higher magnification), and epoxy(32.6)-Ti₃SiC₂(67.4) surface at, (c) lower magnification, (d-e) higher magnification..... 31
10. Figure 10: SE SEM micrographs of, (a) Epoxy(32.6)-Ti₃SiC₂(67.4) and (b) Al₂O₃, (c) Al₂O₃ surface at higher magnifications, and (d) BSE image of the same region. 33
11. Figure 11: Schematics of, (a) IIIa tribofilm, and (b) IVa tribofilm [28]..... 35

ACKNOWLEDGMENTS

I am incredibly grateful to my thesis supervisor Professor Dr. Surojit Gupta for providing me with definite direction, superior guidance, and constant motivation from the beginning of the thesis research as well as encouragement throughout my graduate studies.

In addition I would like to express my sincerest gratitude to my professors at the University of North Dakota for all of the aid and support I received during my studies.

ABSTRACT

The $M_{n+1}AX_n$ (MAX) phases (over 60+ phases) are thermodynamically stable nanolaminates displaying unusual, and sometimes unique, properties. MAX phases are also highly damage tolerant, thermal shock resistant, creep resistant, lubricious, readily machinable, may possess Vickers hardness values of 2–8 GPa, and are anomalously soft for transition metal carbides and nitrides. Because of these properties, there is a huge potential for MAX phase's to improve tribological properties when used in composites. Here for the first time Al, Sn, and Epoxy MAX phase composites will be explored to gain a better understanding of the tribological properties of the various composites.

CHAPTER I

ALUMINUM / MAX PHASE (MAXMET) TRIBOLOGY

INTRODUCTION

The $M_{n+1}AX_n$ (MAX) phases (over 60+ phases) are thermodynamically stable nanolaminates displaying unusual, and sometimes unique, properties [1-14]. These phases are so-called because they possess a $M_{n+1}AX_n$ chemistry, where n is 1, 2, or 3, M is an early transition metal element, A is an A-group element and X is C or N. MAX phases are layered hexagonal (space group $D_{6h}^{4}-P6_3/mmc$) with two formula units per cell. The MAX phases are highly damage tolerant, thermal shock resistant, creep resistant, lubricious, readily machinable, and with Vickers hardness values of 2–8 GPa, are anomalously soft for transition metal carbides and nitrides [1–7, 14]. Some of them are also oxidation resistant [10-13]. Due to the properties mentioned above, there is a huge potential that MAX Phases can be used for different structural applications.

Composites of MAX phases with metals (MAXMET) are important from both a fundamental and an applied perspective. Zhang et al. [15] proposed Ti_3SiC_2 -Cu as a new electro-friction composite material. Gupta et al. [14, 16] developed composites consisting of MAX phases and Ag, which showed solid lubrication over a wide range of temperatures. Anasori et al. [17] reported MAX phase composites with up to 80 vol% Mg are readily machinable, relatively stiff, strong, light, and exhibit ultra

high damping. Increasing the Mg volume fraction leads to lighter composites with higher damping characteristics at lower stresses. Wang et al. [18] fabricated Al-matrix MAXMETs from pure Al and 40 vol% Ti_3AlC_2 powders using a hot isostatic pressing technique. The yield strength of the Al- Ti_3AlC_2 composite was found to be twice that of pure Al [18]. Hu et al. [19] reported that the specific strength of an Al- Ti_2AlC alloy composite was 50% higher than that of peak-aged Al alloy in an interpenetrating 40 vol% - aluminum alloy composite [19]. However, the authors did not investigate the entire spectrum of Al-MAX composites. Recently, Kothalkar et al. [20] reported damping up to 200 MPa higher than any of the metal - MAX phase composites reported in literature for Ti_3SiC_2 (MAX phase) - NiTi (Shape Memory Alloy). Thus, there is a huge potential for multifunctional materials that can be developed using MAX phases as a constituent in Metal Matrix Composites (MMCs) or Ceramic Matrix Composites (CMCs). Although it is well known that Al and Al alloys have poor tribological behavior [21], Al-based MMCs reinforced with rigid ceramic particulates have high specific strength and modulus, good wear resistance, and are easily machinable [22, 23]. They have become increasingly important for structural applications in aerospace, automotive and other transport industries. Due to the incorporation of hard ceramic particles, the machining of MMCs may be difficult, where complex tools are necessary to machine them [24-26].

It is expected; the addition of MAX phases will further enhance the mechanical behavior and machinability of MMCs. The novel MMCs will also have multifunctional attributes, for example, enhanced damping, hardness, and tribological behavior. For rapid usage and fabrication of Al-MAX composites, novel manufacturing methods should be explored. We report for the first time the tribology characterization for novel Al-matrix composites reinforced with Ti_3SiC_2 particulates (nanolaminates).

METHODS

Ti_3SiC_2 powder (Kanthal, Hallstahammar, Sweden) and the tailored concentrations of Al Powder (-325 mesh, Alfa Aesar, Ward Hill, MA) were dry ball milled (8000 M mixer Mill, SPEX SamplePrep, Metuchen, NJ) with polymethyl methacrylate (PMMA) balls for 2 minutes. The mixed powders were then cold pressed in a ~12.7 mm die with a uniaxial compressive stress ~210 MPa. Novel Al-matrix composites were designed with 35 vol% Ti_3SiC_2 (Al(65)- Ti_3SiC_2 (35)), 20 vol% Ti_3SiC_2 (Al(80)- Ti_3SiC_2 (20)), 10 vol% Ti_3SiC_2 (Al(90)- Ti_3SiC_2 (10)), and 5 vol % Ti_3SiC_2 (Al(95)- Ti_3SiC_2 (5)) in an Al matrix. For comparison, pure Al samples were also prepared under similar conditions. Al(65)- Ti_3SiC_2 (35) samples were fabricated by heating the samples at 10 °C/min to 760° C, and then isothermal holding at 760°C for 30 min. All the other compositions were manufactured by heating the samples at 10°C/min to 700 °C, and then isothermal holding at 700 °C for 5 minutes.

For the tribology measurements, all samples were cut into tabs of ~4 mm x ~4 mm x ~3 mm. The samples were then polished until ~1 μm finish. Inconel 718 (California Metals and Supply Inc., Santa Fe Springs, CA) and Al₂O₃ substrates (AL-D-42-2, AdValue Technology, Tucson, AZ) were also polished until ~1 μm finish. A surface profilometer (Surfcom 480A, Tokyo Seimitsu Co. Ltd., Japan) was used to confirm that all surfaces had a R_a < 1 μm.

All tribology studies were then performed using a tab-on-disc tribometer (CSM Instruments SA, Peseux, Switzerland) at loads of 2 N (~0.12 MPa), 5 N (~0.31 MPa), and 10 N (~0.62 MPa) on track radiuses of ~18 mm, ~14 mm, and ~10 mm, respectively. An average of 10 final data points were used to calculate the final friction coefficient (μ_f). The mass of all samples and substrates were measured before and after testing by a weighing scale (Model AL204, Mettler Toledo, Columbus OH). The wear rate (WR) was calculated by using the following equation:

$$WR = (m_i - m_f) / (\rho \cdot N \cdot d) \text{ -----(I)}$$

Where, m_i is the initial mass, m_f is the final mass, ρ is density of the composite, N is the applied load, and d is the total distance traversed by the static partner during testing.

Samples were coated with Au/Pd, using a Balzers SCD 030 sputter coater (BAL-TEC RMC, Tucson AZ USA), and then secured on Al mounts. Secondary Electron (SE) and Backscattered Electron (BSE) images were obtained using a JEOL JSM-6490LV Scanning Electron Microscope (JEOL USA, Inc., Peabody,

Massachusetts). X-ray information was obtained via Thermo NanoTrace Energy Dispersive X-ray detector with NSS-300e acquisition engine. It is important to note at this juncture that the accuracy of measuring Carbon is quite low in the Energy Dispersive Spectroscopy (EDS). It follows that implicitly, and unless otherwise noted, the compositions listed could very well contain C. This is especially true of sub-stoichiometric oxides. In addition, the chemistry of a region that was deemed chemically uniform at the micron level as quantified by EDS – is designated with two asterisks, as *microconstituent* to emphasize that these areas are not necessarily single phases. The presence of C in these tribofilms is shown by adding {C_x} in the composition [14]. For observing the grains, each sample was etched with Kelly's Reagent for 15 s and then rinsed with water.

XRD measurements were performed on an AXS D8 Bruker X-ray Diffraction System, an x-ray diffractometer equipped with a two-dimensional Hi-Star area detector, video camera / laser alignment system, and a Cu x-ray radiation point source.

DATA AND ANALYSIS

1.1 Tribological Behavior

Tribological behavior of the Al-MAX composites were investigated further. Figure 1(a-e) displays the coefficient of friction (μ) versus the distance profile for various Al-MAX compositions. All compositions were tested against Al₂O₃ substrates at loads of 2N, 5N, and 10N and a velocity of 50 cm/s. In general, during

testing, the μ displayed significant fluctuation, however, the composite ameliorated as the content of Ti_3SiC_2 was increased in the Al matrix.

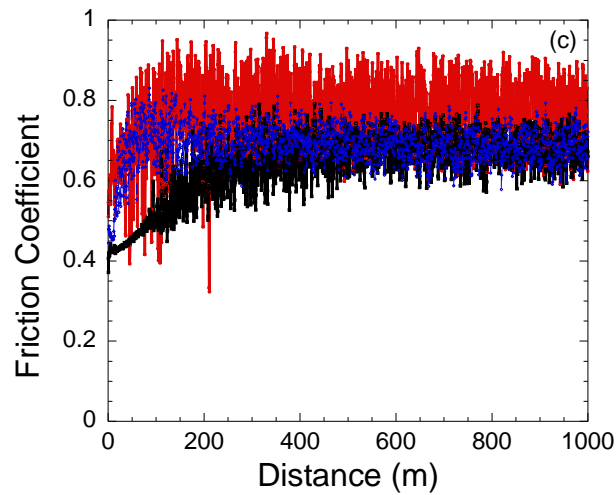
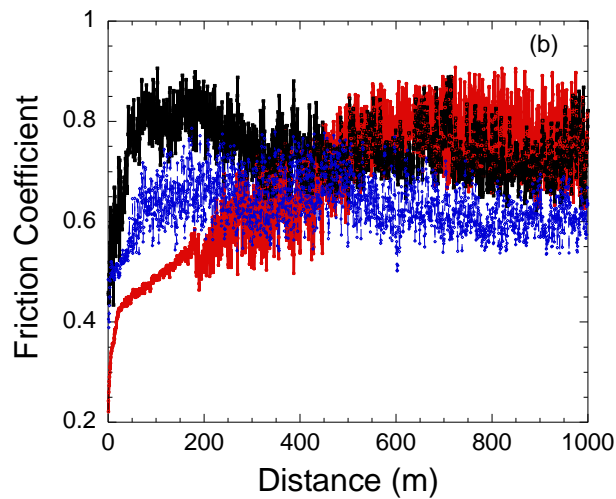
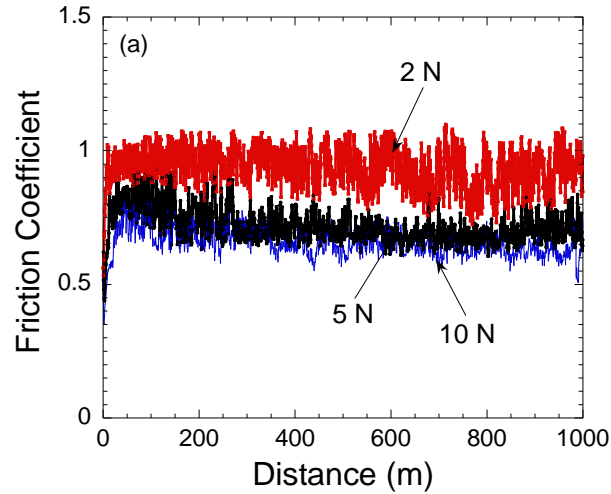


Figure 1 Continued

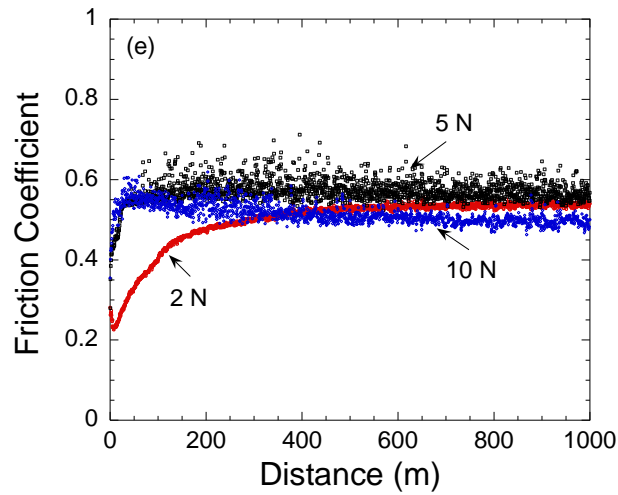
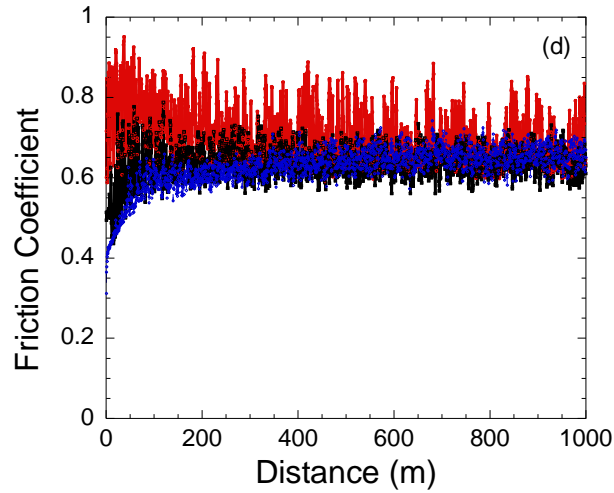


Figure 1: Tribological behavior of, (a) Al, (b) Al(95)-Ti₃SiC₂(5), (c) Al(90)-Ti₃SiC₂(10), (d) Al(80)-Ti₃SiC₂(20), and (e) Al(65)-Ti₃SiC₂(35) against alumina .

For comparison, Figure 2(a) plots the final friction coefficient (μ_f) of all compositions. At a lower stress ~ 0.12 MPa, the μ_f of pure Al was ~ 0.93 , whereas the μ_f of Al(95)-Ti₃SiC₂(5), Al(90)-Ti₃SiC₂(10), and Al(80)-Ti₃SiC₂(20) were ~ 0.76 , ~ 0.74 , and ~ 0.70 , respectively. Comparatively, the μ_f of Al(65)-Ti₃SiC₂(35) was ~ 0.54 , significantly lower than all other compositions tested. However, at higher stresses the μ_f of Al decreased to ~ 0.68 and the μ_f of Al(95)-Ti₃SiC₂(5), Al(90)-Ti₃SiC₂(10), and Al(80)-Ti₃SiC₂(20) samples were comparable to pure Al, but the μ_f of Al(65)-Ti₃SiC₂(35) was ~ 0.50 , and significantly lower.

Figure 2(b) plots the WRs of all compositions. The WRs of all tested composites were similar, and varied between $(2-6) \times 10^{-4}$ mm³/N.m. The WR of pure Al decreased marginally from 5.5×10^{-4} mm³/N.m to 2×10^{-4} mm³/N.m as the normal stress was increased from ~ 0.12 MPa to ~ 0.62 MPa. The WR of all other compositions were similar as the samples were tested at different normal stresses.

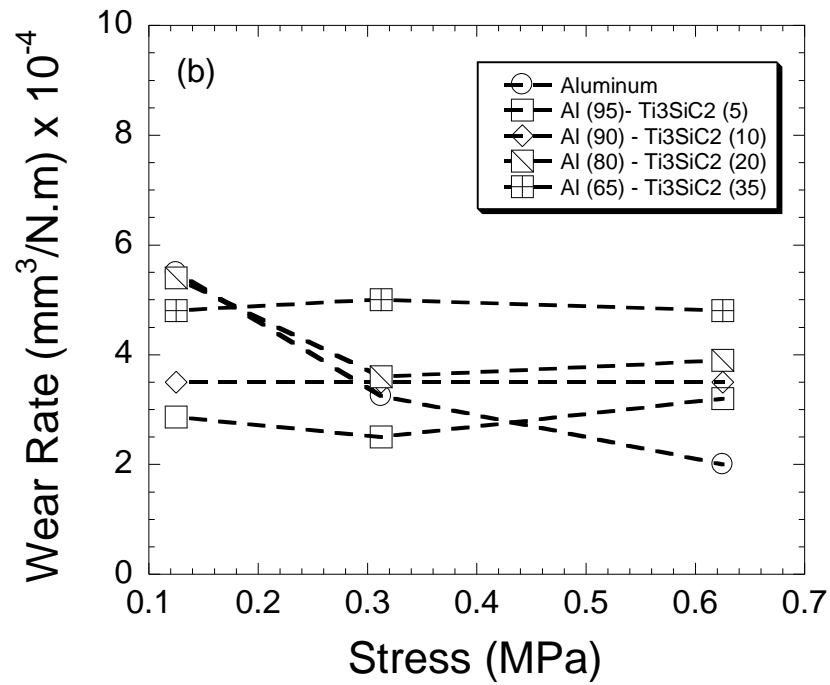
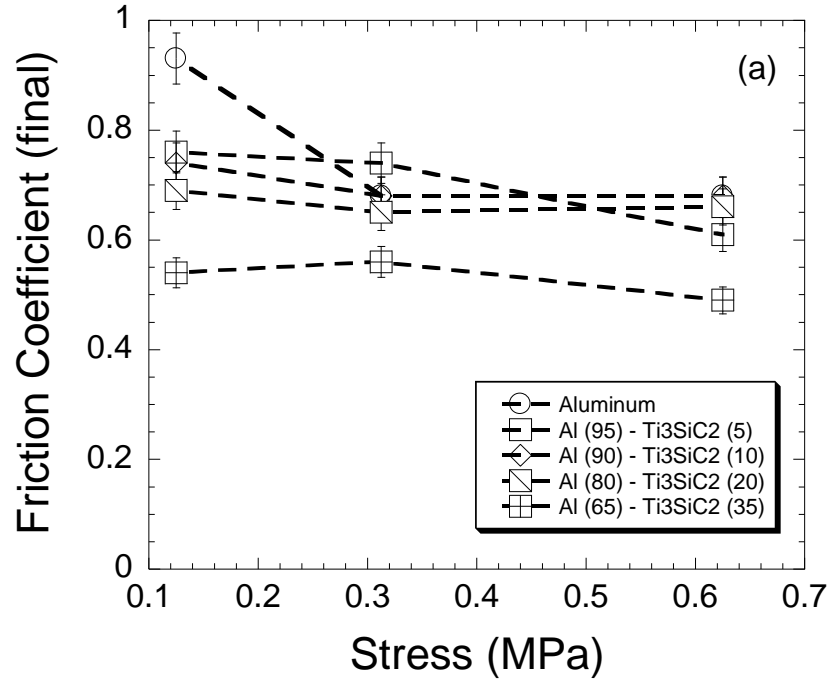


Figure 2: Summary of, (a) Final friction coefficient (μ_f) and (b) Wear Rate (WR).

1.2 Investigation of Tribosurfaces

Figure 3 depicts the tribosurfaces of Al(80)-Ti₃SiC₂(20) and the Al₂O₃ substrate under SE SEM following tribological testing under 5N at 50cm/s at RT. It can be observed that both the Al(80)-Ti₃SiC₂(20) and Al₂O₃ surface are covered with scuffing marks, and powdered third body debris. The EDS analysis of Al(80)-Ti₃SiC₂(20) surface showed microconstituents with *Ti_{0.18}Si_{0.04}Al_{0.5}O_{0.24}{C_x}* (light color) and *Al_{0.34}Si_{0.01}Ti_{0.03}O_{0.63}{C_x}*, (dark color) compositions, respectively.

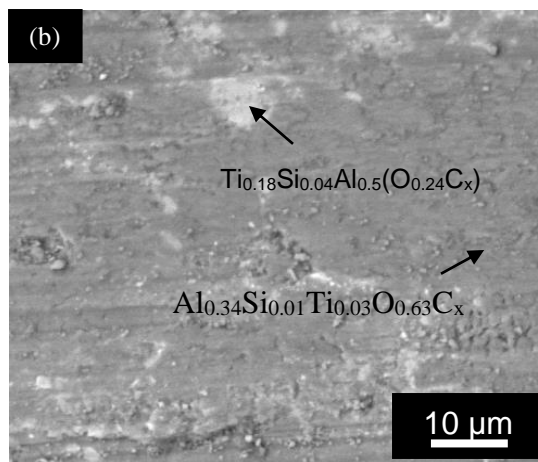
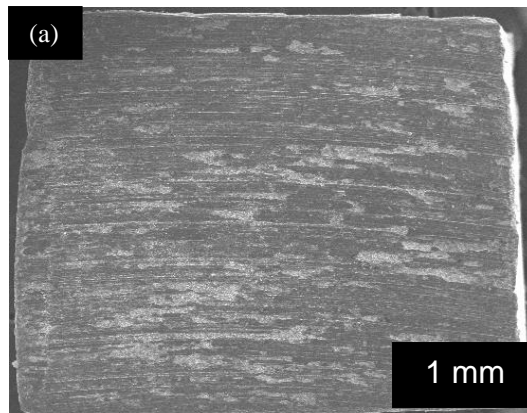


Figure 3 Continued

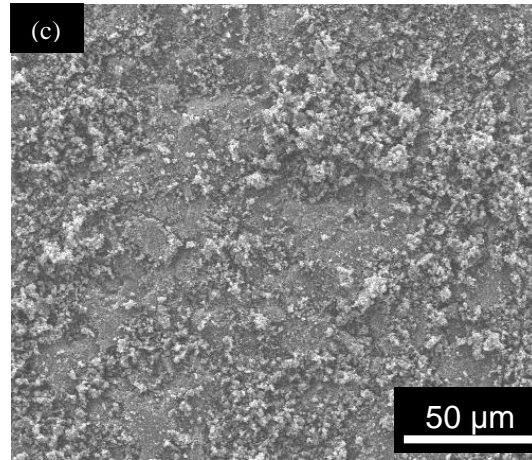


Figure 3: SEM micrographs of, (a) Al(80)-Ti₃SiC₂(20) low, and (b) Al(80)-Ti₃SiC₂(20) high magnification, and (c) Al₂O₃ surface.

1.3 Mechanisms

Recently, Gupta et al. [14] proposed a novel method for classifying tribofilms. A tribofilm can be classified into Type I if triboreactions occur predominantly at the MAX surface; Types II if triboreactions occur at the tribopartner's surface; Types III if both a MAX phase or their composites and the tribopartner contribute to the formation of tribofilms; and Type IV if MAX phase based composites contribute predominantly to the triboreactions. Subsequently, Gupta et al. [14] had divided these categories into sub-categories by taking into account architectures and physical appearance of the tribofilms according to optics and SEM observations. The architectures of the tribofilms were mainly dependent on their degree of oxidation and mechanical integrity like adhesion to the substrate and hardness.

As discussed earlier, only Al-matrix surface is contributing the tribofilms formation, thus the tribofilms formed on the alumina surface can be categorized as Type IV. Gupta et al. [14] had classified Type IV tribofilms in Type IVa and Type IVb. Type IVa tribofilms are visible to the naked eye. They are chemically homogenous at the microscale. It is because of the formation of phases, that the WRs ($\approx 10^{-5}$ mm³/N m) and μ 's (≈ 0.4) were low. Type IVb tribofilms are composed of decomposed Ag-rich regions dispersed with different trioxides. At $\approx 6 \times 10^{-4}$ mm³/N.m the WRs are high, but the μ 's (≈ 0.4) were low. The tribofilms observed during this study are patchy and powdery, thus they do not qualify for either of these categories. They can be further classified as type IVc.

CONCLUSIONS

The authors report for the first time the synthesis and fabrication of Ti₃SiC₂ reinforced Al-matrix composites by pressureless sintering. The addition of Ti₃SiC₂ enhanced the tribological performance of the Al-matrix composite.

CHAPTER II TIN / MAX PHASE (MAXMET) TRIBOLOGY

INTRODUCTION

Multifunctional materials are practical for many applications in materials engineering. Normally, strength is required for load bearing applications to resist wear and conformability, and this combination of properties is achieved by using multilayer structures. It has been proposed by different investigators that Al based alloys with the addition of Sn have enhanced tribological and mechanical properties and are more commonly used in plain bearings, pistons and cylinder liner in internal combustion engines [1-3]. Previous studies have found, in general, Al-Sn alloys possess good antifrictional characteristics; however, due to the soft nature of Sn, there is an inability to support heavy loads [4-5]. Pathak and Mohan did report in a study that there is proportionality between an increase in Sn vol% and a decrease in the μ among alloys [6]. The authors here propose that by introducing much harder MAX phase particles to a Sn based matrix the structural integrity of the material can be enhanced to resist wear from bearing loads. In addition the μ should be reduced as the vol% of MAX phase increases in the Sn matrix composite. It is the author's intentions here to investigate the effects of adding Ti_3SiC_2 particles to a Sn system, and report the tribological benefits of the Sn-MAX composite.

METHODS

Various concentrations of Ti_3SiC_2 (Kanthal, Hallstahammar, Sweden) and Sn Powders (-100 mesh, Alfa Aesar, Ward Hill, MA) were dry ball milled (8000 M mixer Mill, SPEX SamplePrep, Metuchen, NJ) for 2 minutes with PMMA spheres. All compositions were sintered in an ambient atmosphere while hot pressing in a ~25.4 mm die under a uniaxial compressive stress of ~112 Mpa and a temperature of 240°C for 5 minute hold period. All Sn-MAX composites were allowed to reach RT while remaining in the HP at a stress of ~112 Mpa before characterizing any of the materials. The Novel Sn-matrix composites were designed with the addition of 50 vol% Ti_3SiC_2 (Sn(50)- Ti_3SiC_2 (50)), 30 vol% (Sn(70)- Ti_3SiC_2 (30)), 20 vol% (Sn(80)- Ti_3SiC_2 (20)), 10 vol% (Sn(90)- Ti_3SiC_2 (10)), and 5 vol% (Sn(95)- Ti_3SiC_2 (5)) Ti_3SiC_2 into the Sn matrix. For comparison, pure Sn was also fabricated using the same experimental procedure.

To characterize the tribological behavior of the novel Sn composites, all samples were cut into tabs of ~4 mm x ~4 mm x ~3 mm. The cut samples were then polished to a ~1 μm finish. Inconel 718 (California Metals and Supply Inc., Santa Fe Springs, CA) and Al_2O_3 substrates (AL-D-42-2, AdValue Technology, Tucson, AZ) were similarly polished to a ~1 μm surface finish. To confirm all composite samples and substrates had a $R_a < 1\mu\text{m}$, profilometry measurements were completed using a surface profilometer (Surfcom 480A, Tokyo Seimitsu Co. Ltd., Japan). The mass of all samples and substrates were also measured before and after testing using a weighing scale (Model AL204, Mettler Toledo, Columbus OH) for purposes of calculating WR.

All tribology studies were conducted using a tab-on-disc tribometer (CSM Instruments SA, Peseux, Switzerland) under a 5 N (~0.31 Mpa) load, at track radius of ~14 mm. An average of 3 final data points were used to calculate μ_f . The WR was calculated by using equation (I).

All samples were coated with Au/Pd by using a Blazers SCD 030 sputter coater (BAL-TEC RMC, Tucson AZ USA), then secured to Al mounts. SE and BSE images were obtained using a JEOL JSM-6490LV Scanning Electron Microscope (JEOL USA, Inc., Peabody, Massachusetts.) X-ray diffraction information was obtained via a Thermo Nanotrace Energy Dispersive X-ray detector with NSS-300e acquisition engine. It is important to note at this juncture, the accuracy of measuring C is quite low in the EDS. It follows that implicitly, and unless otherwise noted, the compositions listed could very well contain C. This is especially true of sub-stoichiometric oxides. In addition, the chemistry of a region that was quantified chemically uniform at the micron level by the EDS – is designated with two asterisks, as *microconstituent* to emphasize that these areas are not necessarily single phases. The presence of C in these tribofilms is shown by adding {C_x} in the composition [14].

XRD measurements were performed on an AXS D8 Bruker X-ray Diffraction System, an x-ray diffractometer equipped with a two-dimensional Hi-Star area detector, video camera / laser alignment system, and a Cu x-ray radiation point source.

DATA AND ANALYSIS

2.1 Tribological Behavior

The Tribological behaviors of novel Sn-MAX composites are investigated further here. Figure 4(a) exhibits the μ of various Sn matrix composites versus the Sn vol%. It is immediately evident that the concentration of Ti_3SiC_2 directly impacts the μ of the Sn matrix composite. The μ_f of pure Sn, Sn(90)- Ti_3SiC_2 (10), Sn(80)- Ti_3SiC_2 (20), and Sn(70)- Ti_3SiC_2 (30) were 0.72, 0.73, 0.62, and 0.5, respectively. It should be noted that between 70 and 90 vol% of Sn there is a significant increase in μ_f at which point it nearly stabilizes at or around 0.72. Figure 4(b) displays the μ versus the entire 1000m linear sliding distance. Both the pure Sn and Sn(70)- Ti_3SiC_2 (30) composite sample display, increases over the course of the first 300m. It is evident that the introduction of Ti_3SiC_2 to the pure Sn decreased the initial spike from ~ 0.65 to ~ 0.5 , respectively. Following the initial 300m the Sn(70)- Ti_3SiC_2 (30) composite sample's μ also remained more stable than the erratic pure Sn sample. Lastly, the pure Sn sample revealed a significantly higher μ_f than the Sn(70)- Ti_3SiC_2 (30). Thus indicating that the addition of Ti_3SiC_2 to an Sn matrix proves to be beneficial for tribological purposes.

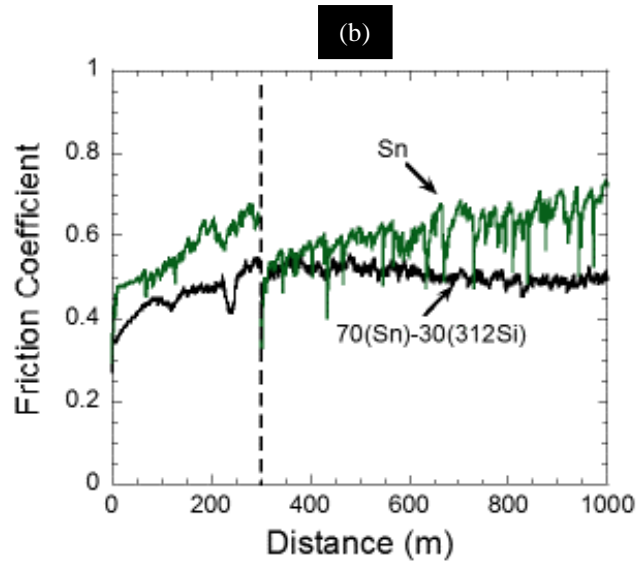
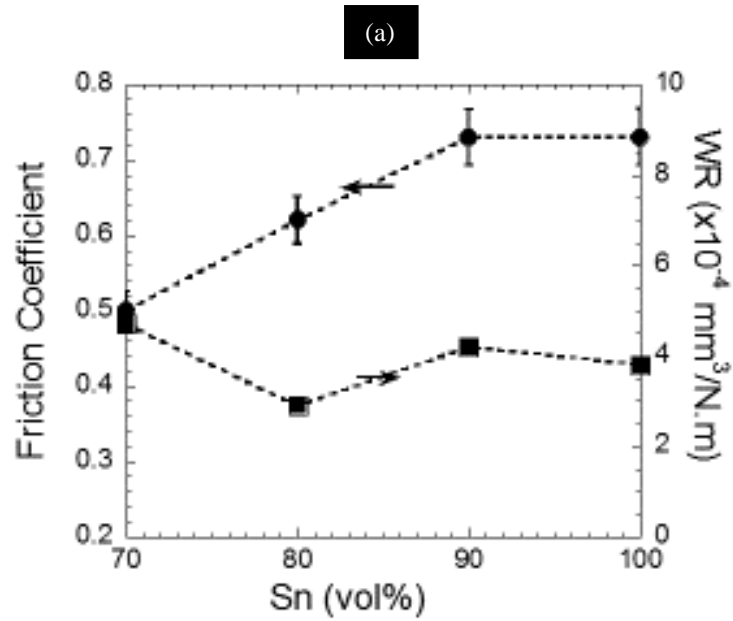


Figure 4: Plot of, (a) Coefficient of friction and Wear Rate Versus Vol% of Ti_3SiC_2 additions in a Sn matrix, and (b) Coefficient of Friction versus distance of Sn(70)- Ti_3SiC_2 (30) and Sn samples against alumina.

Figure 4(a) also plots the WRs of all Sn composite compositions. The WRs of all tested composites were similar, and varied between $(3-5) \times 10^{-4} \text{ mm}^3/\text{N.m}$ under a normal 5N load. Although the WR varied slightly between the pure Sn sample and the Sn(70)-Ti₃SiC₂(30) composite, the variances are nearly negligible. Further testing should be completed in the future to understand how the WR would behave with less than 70 vol% Sn to have a more conclusive understanding of how the addition of Ti₃SiC₂ would affect Sn on a broader spectrum.

2.2 Investigation of Tribosurfaces

Figure 5 (a-d) depicts the tribosurfaces of Sn(70)-Ti₃SiC₂(30) and the Al₂O₃ substrate under SE SEM following tribological testing under a 5N load at 50cm/s in ambient temperature condition. It can be observed that both the Sn(70)-Ti₃SiC₂(30) and Al₂O₃ surface is covered with scuffing marks, and powdered third body debris. The EDS analysis of Sn(70)-Ti₃SiC₂(30) surface showed microconstituents with $*(\text{Sn}_{0.6}\text{Ti}_{0.3}\text{Si}_{0.1})\text{O}_{0.8}\{\text{C}_x\}$ * (light color).

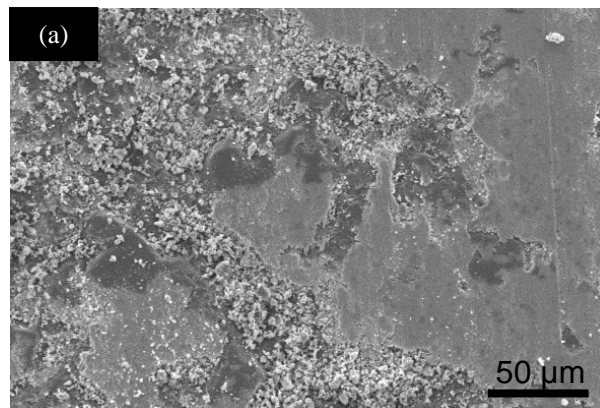


Figure 5 Continued

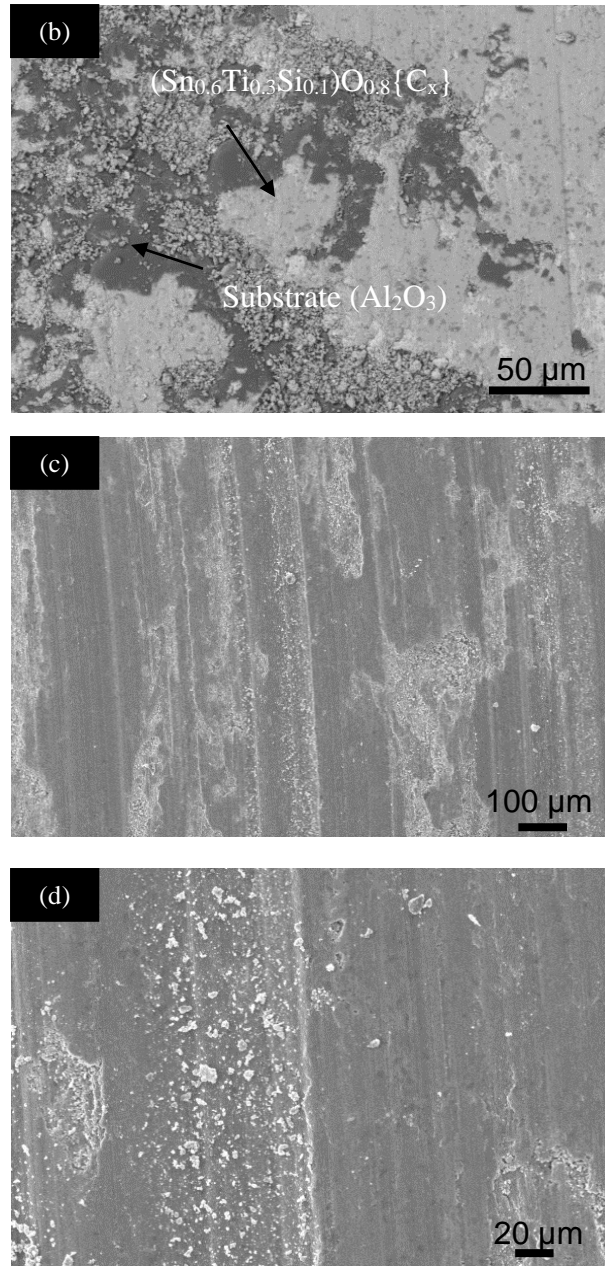


Figure 5: SE SEM micographs of, (a) Al_2O_3 Substrate (low magnification), and (b) Al_2O_3 Substrate (high magnification), (c) Sn(70)- Ti_3SiC_2 (30) and, (d) BSE image of the same surface.

Figure 5(a-d) shows the SEM micrographs of the Sn(70)-Ti₃SiC₂(30) and Al₂O₃ surfaces after testing. It is evident by examining Figure 5(c-d) that surface wear scars are present on the surface of the Sn(70)-Ti₃SiC₂(30) composite, whereas, several patches of tribofilms were observed (Fig. 5(a-b)) on the Al₂O₃ surface. Figures 5(a-b) show the morphology of tribofilms at a higher magnification. Clearly, the transfer films are formed due to a mild tribooxidation and wear from the Sn(70)-Ti₃SiC₂(30) surface.

CONCLUSIONS

The authors of this study report the successful synthesis and fabrication of novel Ti₃SiC₂ reinforced Sn-matrix composites by uniaxial hot pressing. The addition of Ti₃SiC₂ enhanced the coefficient of friction during tribological studies but had nearly negligible effects on the WR.

CHAPTER III EPOXY / MAX PHASE (MAXPOL)

INTRODUCTION

It has previously been explained that MAXMETs play a significant role from both a fundamental and an applied perspective. Gupta et al. [1-8] has comprehensively studied the tribology of MAX phases and their composites. As a part of his previous study, the authors demonstrated that MAX phase-based composites can be used as shafts against Super Alloy (SA) foils for different foil bearing applications at 50,000rpm from RT up to 550°C during thermal cycling [9]. Earlier, despite several years of research there were no structural materials, which could be used as a solid lubricant in temperatures ranging from RT to 550°C [10,11]. Thus, there is a huge potential for materials that can be used in different tribological and engineering systems, e.g., air-foil bearings, gas turbine seals, cylinder wall/piston ring lubrication for low-heat rejection diesel engines, various furnace components, among many others [1]. By manufacturing composites with hexagonal metals, it is also possible to enhance the damping behavior of these materials [12-14]. Recently, Ansari et al. [14] fabricated readily machinable, relatively stiff, strong and light MAX-Mg composites with ultra high damping, where ~30% of the mechanical energy is dissipated at 250 MPa.

Polymers and their composites are currently used extensively in aerospace, automobile, and chemical sectors due to their low density, excellent strength to weight ratios, resistance to corrosion, self lubricating properties, low μ and better wear resistance, and in some cases, provide an alternative to metallic materials

[15-23]. Generally, ceramic particles are added to a polymer matrix to enhance the mechanical and tribological performance [17-20]. Unfortunately, there has been no exploratory research on the design of MAX-Polymer (MAXPOL) composites. Here, we report for the first time the synthesis and characterization of Epoxy-Ti₃SiC₂ composites.

METHODS

During this study three different compositions of epoxy matrix reinforced composites with 20.7 vol% (epoxy(20.7)-Ti₃SiC₂(79.3), 32.6 vol% (epoxy(32.6)-Ti₃SiC₂(67.4)), and 71.6 vol% (epoxy(71.6)-Ti₃SiC₂(28.4)) were manufactured for the first time. For comparison, a pure epoxy sample was also prepared under similar conditions.

The base epoxy samples were fabricated by mixing ~0.9 g hardener (West System 206 Slow Hardener, Gougen Brothers, Inc. Bay City, MI) and ~4.5 g epoxy resin (West System 105 Epoxy Resin, Gougen Brothers, Inc. Bay City, MI) with a wooden spatula by hand, stirring for ~1 min. Thereafter, the composition was cast in ~25 mm plastic molds. All compositions were fabricated by mixing the Ti₃SiC₂ powders (-325, Kanthal, Hallstahammar, Sweden) with the epoxy composition as described above. The final fabrication process was different for the composite samples.

The epoxy(20.7)-Ti₃SiC₂(79.3) composition was cast by the method described above. Both the epoxy(32.6)-Ti₃SiC₂(67.4) and epoxy(71.6)-Ti₃SiC₂(28.4) compositions were too viscous to be manually cast. The epoxy(32.6)-Ti₃SiC₂(67.4) composition was cast in ~25 mm molds by applying vibration during casting.

The epoxy(71.6)-Ti₃SiC₂(28.4) composite was fabricated by cold pressing the mixture in ~12.5 mm dies while applying an uniaxial stress of ~105 MPa. The relative volume fraction of polymer in the epoxy(71.6)-Ti₃SiC₂(28.4) composite was accurately determined by baking the composite in a tube furnace at 400 °C for 4 h in an Inert Ar environment. The weight analysis showed that the composites have ~71.6 vol% Ti₃SiC₂. All compositions were cured for 24 h under ambient conditions.

Samples were secured to Al mounts and coated with gold/palladium using a Balzers SCD 030 sputter coater (BAL-TEC RMC, Tucson AZ). SE and BSE Images were obtained by using a JEOL JSM-6490LV Scanning Electron Microscope (JEOL USA, Inc., Peabody, Massachusetts). X-ray information was obtained via a Thermo Nanotrace Energy Dispersive X-ray detector with NSS-300e acquisition. It is important to note at this juncture that the accuracy of measuring Carbon is quite low in the EDS. It follows that implicitly, and unless otherwise noted, the compositions listed could very well contain C. This is especially true of sub-stoichiometric oxides. In addition, the chemistry of a region that was deemed chemically uniform at the micron level as quantified by EDS – is designated with two asterisks, as *microconstituent* to emphasize that these areas are not necessarily single phases.

The presence of C in these tribofilms is shown by adding {C_x} in the composition [1].

For all tribology measurements, the samples were cut into tabs of ~4 mm x ~4 mm x ~3 mm. The samples were then polished until ~1 μm finishing. Inconel 718 (California Metals and Supply Inc., Santa Fe Springs, CA) and Al₂O₃ substrates (AL-D-42-2, AdValue Technology, Tucson, AZ) were also polished until ~1 μm finish. Using a surface profilometer (Surfcom 480A, Tokyo Seimitsu Co. Ltd.,

Japan), it was confirmed that all samples had a $R_a < 1 \mu\text{m}$. The tribology studies were then performed using a tab-on-disc tribometer (CSM Instruments SA, Peseux, Switzerland) with a 5 N ($\sim 0.3 \text{ MPa}$) load, 50 cm/s linear speed, and $\sim 9 \text{ mm}$ track radius.

The mass of the samples and substrates were measured before and after testing using a weighing scale (Model AL204, Mettler Toledo, Columbus OH). The WR was calculated using Equation (I).

DATA AND ANALYSIS

3.1 Tribological Behavior

Figure 6 shows the variation of μ versus distance profiles for the various Epoxy- Ti_3SiC_2 composites against Inconel 718 and Al_2O_3 . In both cases, the μ decreased as the concentration of Ti_3SiC_2 was increased. Comparatively, the μ displayed higher fluctuation during testing against Inconel 718 (Figs. 6(a-b)) as compared to Al_2O_3 (Fig. 6(c-d)). However, in both cases the initial μ had a lower value before reaching a steady state. Different research groups have observed similar transitions during tribological studies of MAX phases against various tribopartners [4-6, 24]. The initial low μ region is commonly referred to as Regime I, and the high μ region is referred as Regime II. Figure 7 shows a typical behavior of Ti_3SiC_2 sliding

against Inconel 718 [6]. Where regime I and II is accompanied by low WR and high WR, respectively.

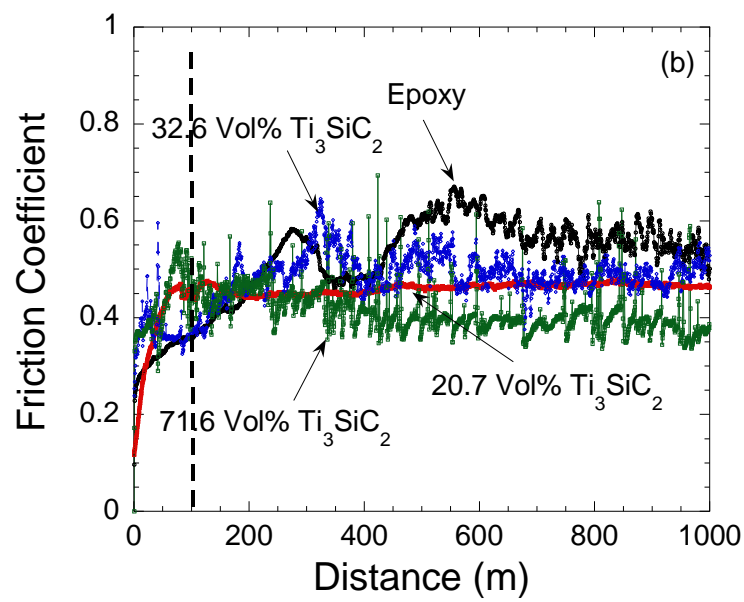
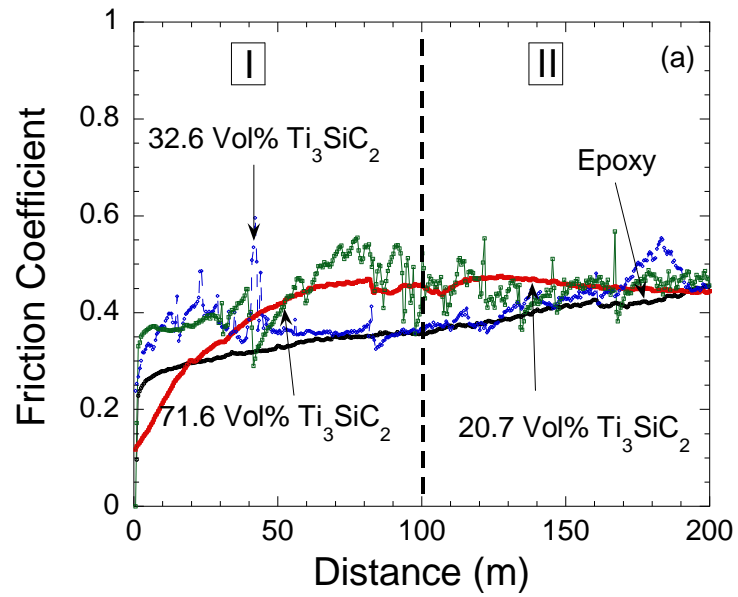


Figure 6 Continued

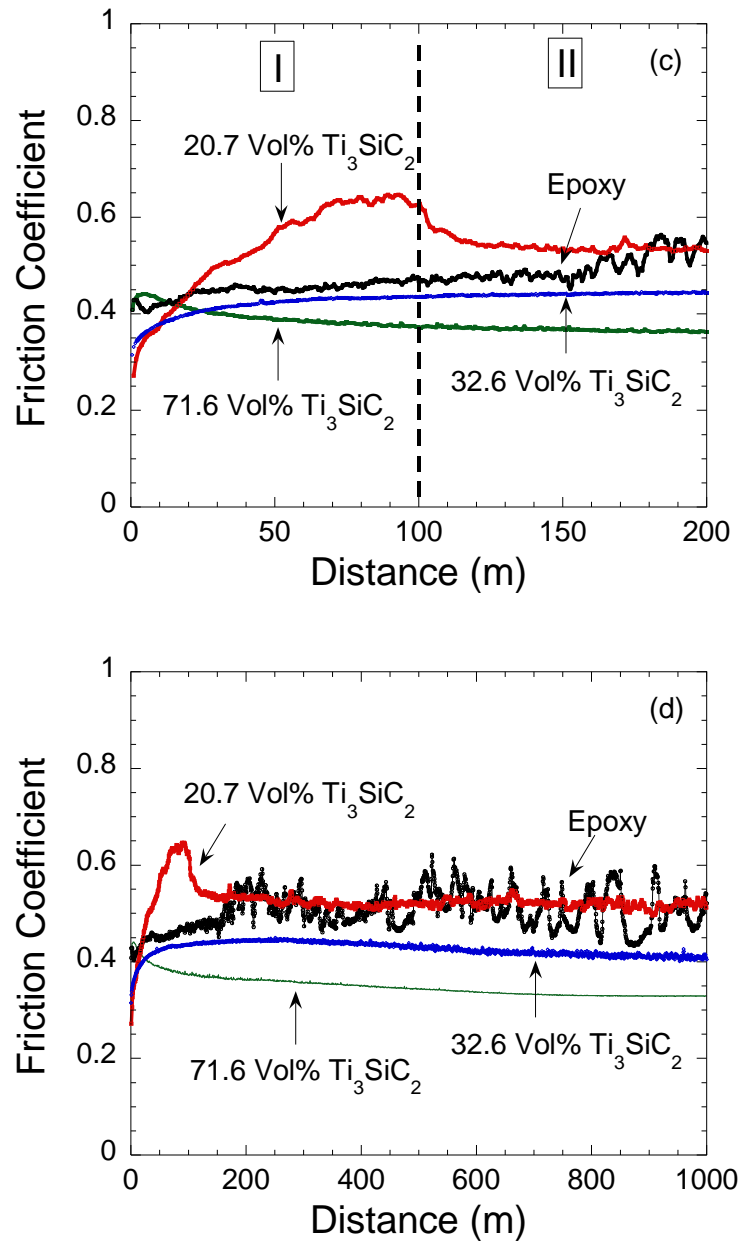


Figure 6: Tribological behavior of Epoxy- Ti_3SiC_2 against, (a) Inconel 718 (first 200 m), (b) Inconel 718, (c) alumina (first 200 m), and (d) alumina.

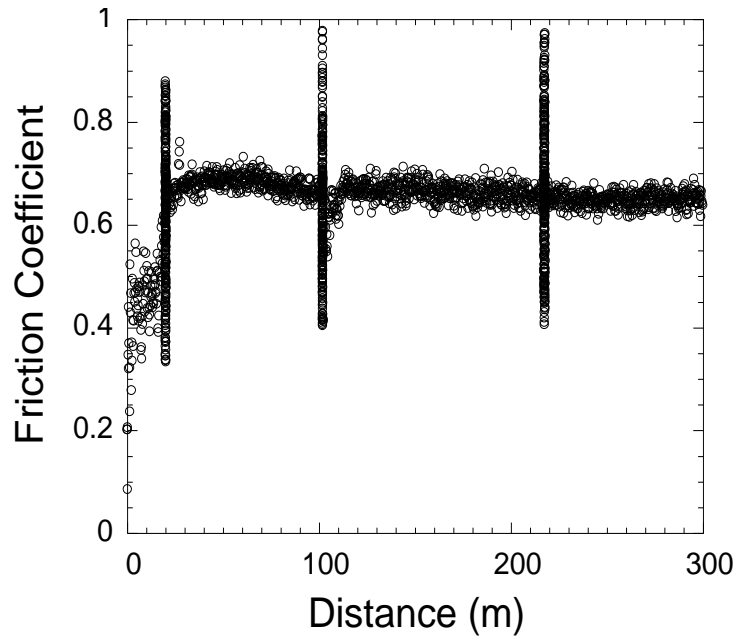


Figure 7: Change in μ as a function of sliding distance when Ti_3SiC_2 was tested against Inconel 718 [25].

From this study, the following observations can be made: (a) addition of Ti_3SiC_2 decreased μ , (b) in all of the composite samples, the transition from regime I to regime II happened within the first ~100 m of dry sliding, (c) addition of Ti_3SiC_2 in epoxy accelerated the transition to regime II as compared to the baseline epoxy samples, and (d) during this tribological study of epoxy(71.6)- Ti_3SiC_2 (28.4) and epoxy(32.6)- Ti_3SiC_2 (67.4) against Al_2O_3 , the μ decreased slowly during regime II. The last observation shows that the addition of Ti_3SiC_2 in an epoxy matrix makes the structure self lubricating.

Figures 8(a-b) display plots of the μ_{mean} (Y1 axis) and WRs (Y2 axis) versus Ti_3SiC_2 concentration against Inconel 718 and Al_2O_3 substrates, respectively. In both cases, μ_{mean} decreased as the concentration of Ti_3SiC_2 in the epoxy matrix was increased. Interestingly, μ_{mean} was higher against Inconel 718 as compared to Al_2O_3 . For example, μ_{mean} of Epoxy(32.6)- Ti_3SiC_2 (67.4) was 0.42 ± 0.01 and 0.48 ± 0.05 against Al_2O_3 and Inconel 718, respectively. Clearly, the addition of Ti_3SiC_2 decreased the μ and the composites exhibited a self lubricating behavior.

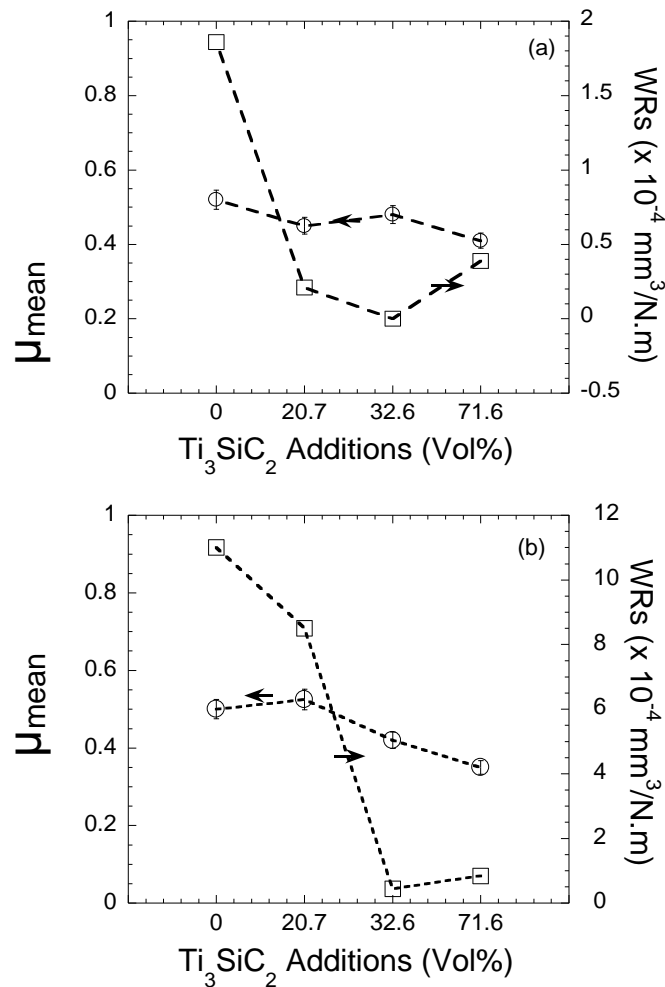


Figure 8: Summary of tribological behavior of Ti_3SiC_2 -epoxy composites against, (a) Inconel 718, and (b) alumina substrates.

The concomitant WRs also decreased steadily (the plots only show the WRs of static partners as the WRs of the dynamic partner were negligible), and then increased slightly after reaching a concentration of ~32.6 vol% Ti_3SiC_2 against both the substrates (Fig.8). For example, during tribology studies against Inconel 718, the WRs decreased significantly from $\sim 1.86 \times 10^{-4} \text{ mm}^3/\text{N.m}$ for pure epoxy samples to $\sim 2.1 \times 10^{-5} \text{ mm}^3/\text{N.m}$ in epoxy(20.7)- Ti_3SiC_2 (79.3) samples, thereafter, the WRs further decreased and became negligible in epoxy(32.6)- Ti_3SiC_2 (67.4), then increased slightly to $\sim 3.9 \times 10^{-5} \text{ mm}^3/\text{N.m}$ (Fig. 9a). The corresponding WRs of Inconel 718 against pure epoxy, epoxy(20.7)-(79.3) Ti_3SiC_2 , and epoxy(32.6)- Ti_3SiC_2 (67.4) was negligible. The Inconel 718 substrate against epoxy(71.6)- Ti_3SiC_2 (28.4) had a low WR of $1.2 \times 10^{-5} \text{ mm}^3/\text{N.m}$.

Comparatively during tribological studies against Al_2O_3 , the WR decreased from $11 \times 10^{-4} \text{ mm}^3/\text{N.m}$ in pure epoxy to $8.5 \times 10^{-4} \text{ mm}^3/\text{N.m}$ in epoxy(20.7)- Ti_3SiC_2 (79.3), and then dropped to $4.4 \times 10^{-5} \text{ mm}^3/\text{N.m}$ in epoxy(32.6)- Ti_3SiC_2 (67.4) (Fig. 9b), the WR slightly increased to $8.4 \times 10^{-5} \text{ mm}^3/\text{N.m}$ in the epoxy(71.6)- Ti_3SiC_2 (28.4) samples. From these observations, we can conclude that the addition of Ti_3SiC_2 enhances the wear resistance of the Epoxy- Ti_3SiC_2 composites.

For comparison, the WR of Ti_3SiC_2 during tribological testing against Inconel 718 was $\sim 2.5 \times 10^{-2} \text{ mm}^3/\text{N.m}$, and the WR of Ta_2AlC (authors could not find data on Ti_3SiC_2 -alumina tribocouples under similar conditions) against alumina was $\sim 2 \times 10^{-2} \text{ mm}^3/\text{N.m}$ [5].

3.3 Investigation of Tribosurfaces

Figure 9 shows SEM micrographs of the Inconel 718 substrate and the epoxy(32.6)-Ti₃SiC₂(67.4) counterpart surfaces after testing. No significant mass transfer was observed on either surface. A few locations on the epoxy(32.6)-Ti₃SiC₂(67.4) surface displayed scuffing marks. Wear debris was observed within these marks. The averaged EDS reading of a microconstituent for a region of wear debris was $*(Ni_{0.20}Cr_{0.13}Fe_{0.08}Ti_{0.18}Si_{0.04})O_{0.43}C_x*$. From these observations, we can conclude that mild oxidation and wear on both surfaces are taking place due to triboreactions.

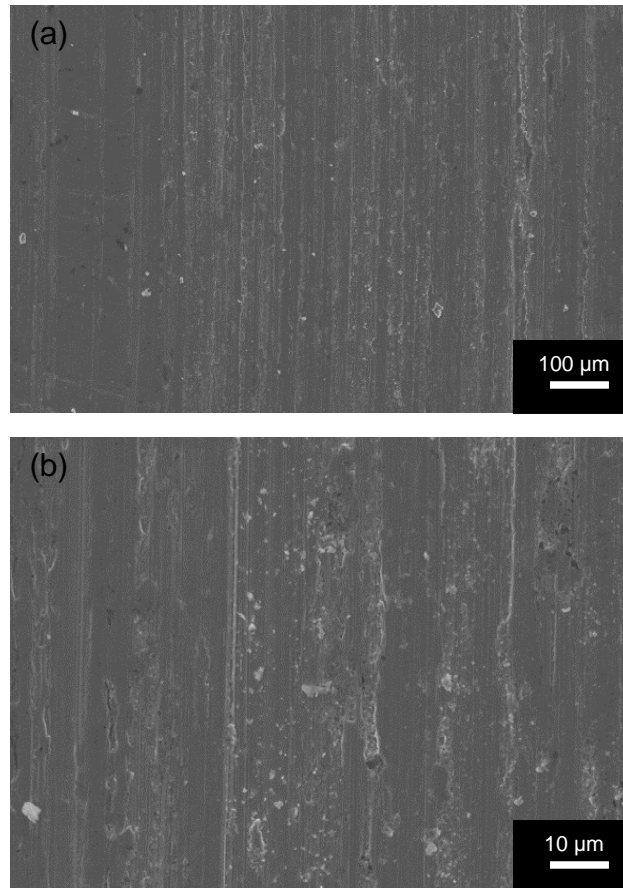


Figure 9 Continued

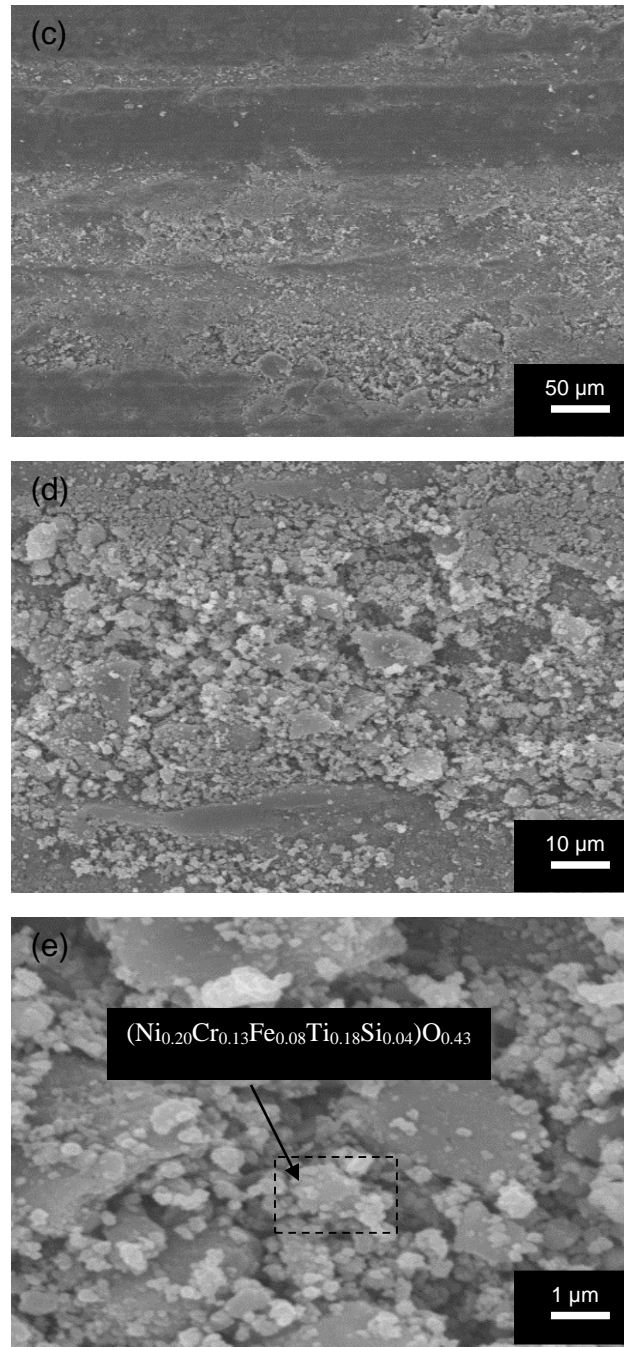


Figure 9: SE SEM micrographs of, (a) Substrate (lower magnification), (b) Substrate (higher magnification), and epoxy(32.6)-Ti₃SiC₂(67.4) surface at, (c) lower magnification, (d-e) higher magnification.

Figure 10 shows the SEM micrographs of the epoxy(32.6)-Ti₃SiC₂(67.4) and Al₂O₃ surfaces after testing. It is evident by examining Figure 10(a) that surface wear scars are present on the surface of the epoxy(32.6)-Ti₃SiC₂(67.4) composite, whereas, several patches of tribofilms were observed (Fig. 10b) on the Al₂O₃ surface. Figures 10(c-d) show the morphology of tribofilms at a higher magnification. The averaged EDS reading of a microconstituent region was *(Ti_{0.36}Si_{0.12}Al_{0.01})O_{0.5}C_x*. Clearly, the transfer films are formed due to a mild triboxidation and wear from the epoxy(32.6)-Ti₃SiC₂(67.4) surface.

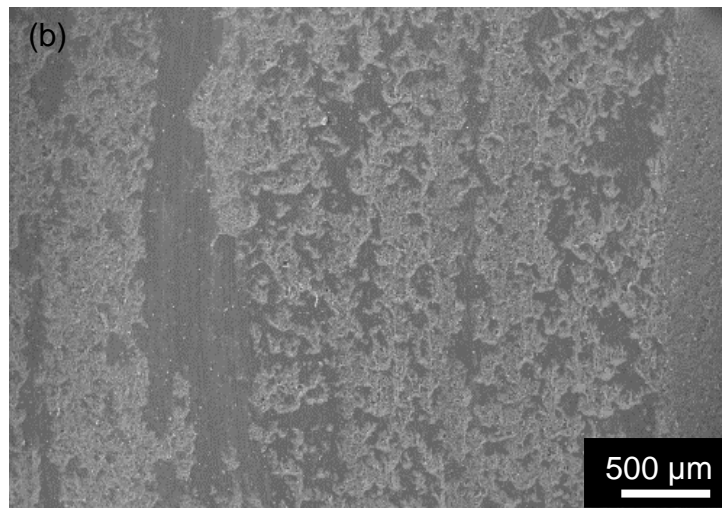
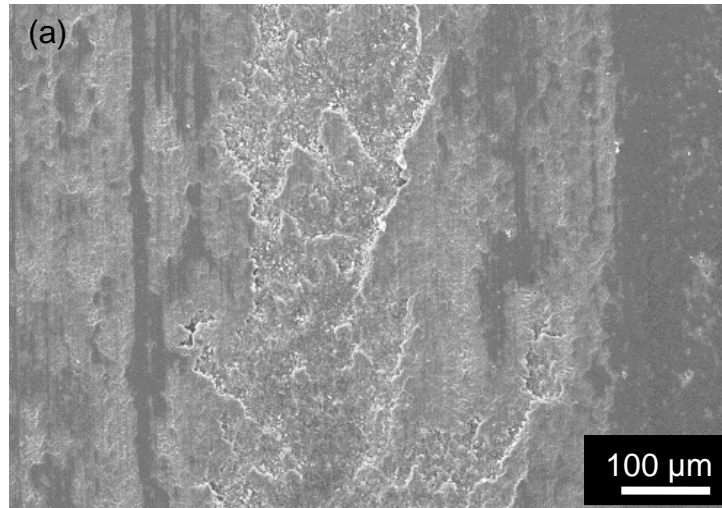


Figure 10 Continued

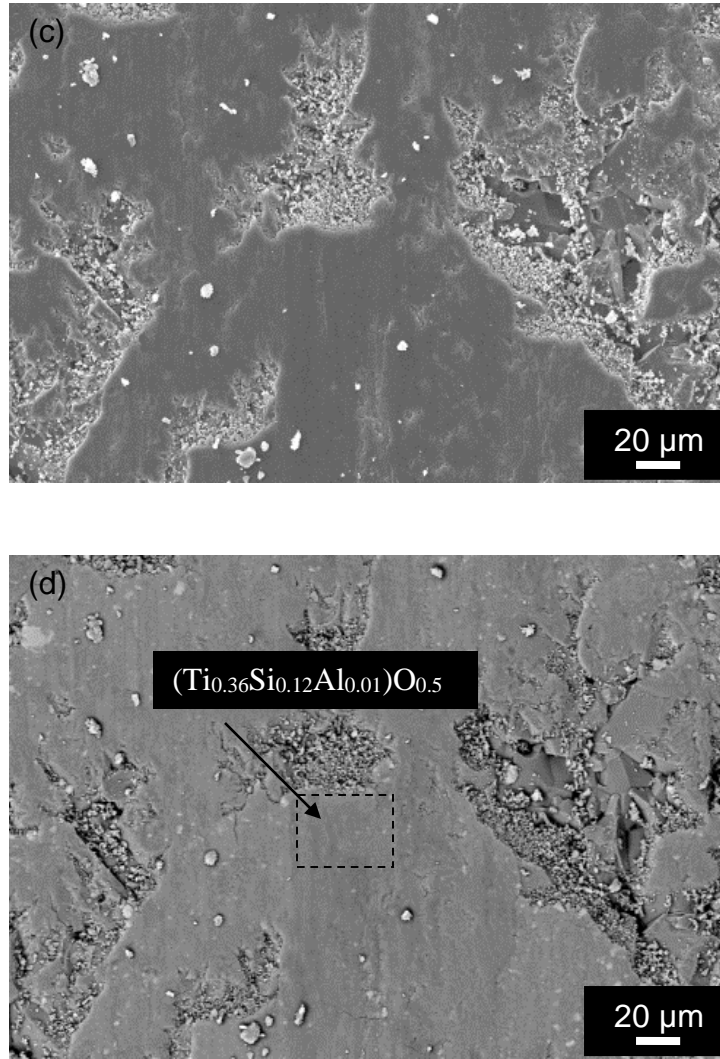


Figure 10: SE SEM micrographs of, (a) Epoxy(32.6)-Ti₃SiC₂(67.4) and (b) Al₂O₃, (c) Al₂O₃ surface at higher magnifications, and (d) BSE image of the same region.

3.4 Fundamental Mechanisms

As mentioned earlier, during the first report on synthesis and characterization of Ti_3SiC_2 , the Ti_3SiC_2 felt lubricious [2]. It led Myhra et al. [6] to study its tribological properties by using a lateral force microscope with a Si_3N_4 tip. They showed that indeed the μ of the basal planes were ultra-low ($2-5 \times 10^{-3}$). The μ of non-basal planes, however, were much higher. The low friction was also quite robust vis-à-vis exposure to the atmosphere. As discussed earlier, the tribology of MAX phases on a macroscale is complex and there is duality during the tribology testing of Ti_3SiC_2 [1, 27-28]. It is not yet clear what causes this duality in tribological behavior. Souchet et al. [28] proposed that it was caused by the creation, and subsequent microcracking or micro-gouging, of an oxy-carbide layer. The observance of pulverized oxy-carbide particles on the various MAX phases tested at room temperature indirectly supports this argument [1, 26-28]. The exact mechanism responsible for the microcracking is still unclear. A more detailed study on the step-by-step evolution of the oxy-carbide layer, its subsequent delamination and microcracking, are needed to better understand this dual-regime in μ . Nevertheless, it is reasonable to conclude that microcracking of these partially oxidized layers generate third body particles, which, in turn, are most probably responsible for the high WRs at room temperature.

By using Gupta's et. al. [1] method of classifying tribofilms, it can be noted that tribofilms formed on the epoxy(32.6)- Ti_3SiC_2 (67.4) surface can be classified as Type IIIa. The tribofilms were barely visible to the naked eyes and amorphous thin layers were observed over each tribosurface by the SEM [33]. Figure 11(a) shows the schematics of type IIIa tribofilms.

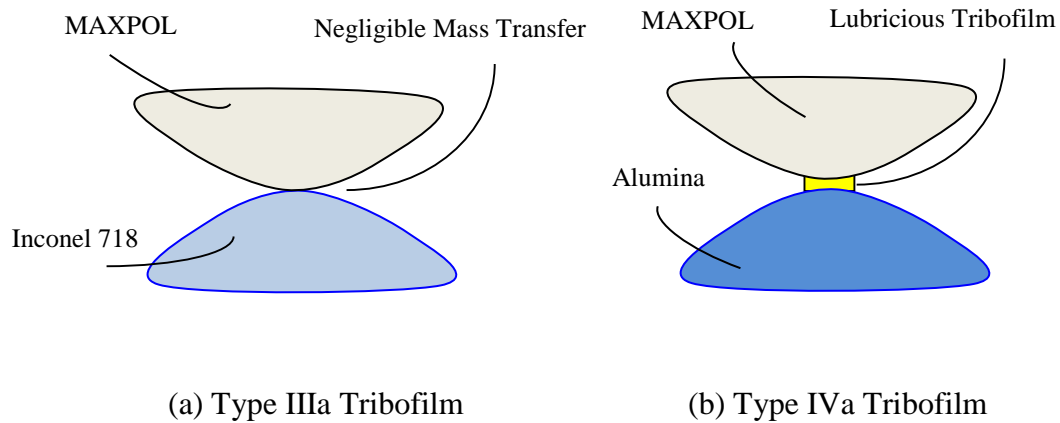


Figure 11: Schematics of, (a) IIIa tribofilm, and (b) IVa tribofilm [28].

Tribofilms formed on the Al_2O_3 substrate surface during dry sliding against epoxy(32.6)- Ti_3SiC_2 (67.4) can be classified as Type IVa, since the tribofilm was lubricious and no phase separation was observed in the microscale [1]. Gupta et al. [1, 7] studied the tribological behavior of Ta_2AlC sintered with 20 vol% Ag (TaAg11) against Inconel 718 and Al_2O_3 . When the TaAg11 composites were tested against Inc718 under a 3N load at room temperature, μ was initially ~ 0.1 , before gradually increasing to ~ 0.6 [1, 7]. However, against Al_2O_3 the μ 's were initially low, but increased gradually to ~ 0.35 . After 2 km sliding distance at room temperature, the WR of TaAg11 samples were $\sim 2 \times 10^{-5} \text{ mm}^3/\text{N.m}$. A similar WR was observed when it was tested against Al_2O_3 [1, 7]. Gupta et al. [1, 7] postulated that the formation of Ag rich phases at the grain boundaries seem to prevent the formation of large abrasive wear particles, which in turn reduces the WR by 3 orders of magnitude. Gupta et al. [1] also hypothesized that the above-

mentioned factor is the key in preventing high WRs: the MAX phase grains have to be prevented from pulling out.

In the present study, epoxy present at the phase boundaries prevented the pull out of MAX phase particles. This is the first study to confirm that Ti_3SiC_2 particles can act as a source of solid lubricant in an epoxy matrix. Consequently, novel MAXPOL composites can be fabricated for multifunctional applications.

CONCLUSIONS

Epoxy- Ti_3SiC_2 composites were synthesized and tested for their tribological behavior for the first time. The mean coefficient of friction decreased during tribological testing against Inconel 718 and Al_2O_3 substrates as the concentration of Ti_3SiC_2 in the epoxy matrix was increased. Against both substrates, the concomitant WRs also decreased steadily, and then increased slightly after reaching a concentration of ~32.6 vol% Ti_3SiC_2 . The tribofilms formed on the Al_2O_3 substrate surface during dry sliding of Epoxy(32.6)- Ti_3SiC_2 (67.4) can be classified as Type IVa as the tribofilm was lubricious and no phase separation was observed on the microscale [28].

The tribofilms formed on epoxy(32.6)- Ti_3SiC_2 (67.4) surfaces can be classified as Type IIIa as the tribofilms were barely visible to the naked eyes and amorphous thin layers over each tribosurface were observed via SEM. The tribological studies prove that the addition of Ti_3SiC_2 in the epoxy matrix imparts self lubricity to the composites.

CHAPTER IV

FUTURE WORK

Zinc (Zn) is one of the most common elements found in the earth's crust and is also present in soil, air, water, and all foods eaten today [1]. Due to Zn's abundance, it has been of great interest for many years in the field of Materials Engineering. Currently there are many uses for Zn in industry. A common practice used today is to coat steel, iron, as well as other metals to prevent rust and corrosion; this process is referred to as galvanization. Zn is also commonly paired with other metals to form alloys such as brass and bronze [2].

It should be to no surprise that due to the significant role Zn currently plays in industry there is an increasing interest in using Zn as the leading constituent in MMCs. The demand for MMCs is driven by industries need for wear resistant, lightweight, stiff and strong materials [3]. Wear is one of the most commonly encountered industrial problems leading to the replacement of components and assemblies in engineering [4]. Due to the significant role wear plays in the field of engineering it will be of the most interest here.

Wear leads to a significant number of operating inefficiencies in engineering assemblies. Though rarely catastrophic, increasing power losses and component replacement have grabbed the attention of engineers to decrease such problems. MMCs have become a very attractive alternative solution in recent years because of their potential advantages over monolithic alloys. MMCs are most commonly reinforced with

high strength, high modulus, and hard second phase brittle ceramics in the form of fibre, whiskers, or particulates [5]. With the addition of ceramic reinforcements to a metal matrix the strength, stiffness and abrasion resistance are increased. However, this comes at the expense of the materials ductility.

In a study conducted by Prasad [6], a Zn based alloy (Zn-37.2% Al-2.5% Cu-0.2% Mg) and the same Zn alloy with 10 wt.% SiC particles dispersed in it were compared using an abrasion tester. It was determined from this test that the hard secondary phases in the composite resisted the penetrating action of the abrasive medium, and therefore, protected the relatively softer matrix surrounding the hard phases, on the specimen's surface. It was also determined from this study that the hard secondary particles are subjected to microcracking followed by fracture and/or removal. The extent of damage to the specimen surface and the abrasive particles in this test is directly related to the hardness and particle size. Also of great significance from this study, it was determined that the matrix of the alloy gets work hardened in due course of abrasion and causing the wear rate of the specimen to decrease; this assists considerably in maintaining the integrity of the composite. However, the work hardened layer increases in thickness with the sliding distance. After attaining a critical thickness the work-hardened layer cracks and disintegrates the work hardened layer causing an increase in wear. It was concluded, the resistance offered by the reinforcement phase by way of its retention on the wear surface reduces the overall wear rate and wear rates in this study we found to be as low as $10^{-11} \frac{m^3}{m}$ [6].

Zn-Al alloys have also been investigated to great lengths recently in an attempt to replace more traditional bearing materials, including but not limited to bronze, cast iron, steel, and plastics. This has been of increasing interest since recent testing has indicated Zn-Al alloys have produced high resistance to wear, high strength, low density, low cost, and low coefficient of friction. A major problem cited with Zn-Al alloys refers to the dimensional instability, which is caused by the presence of metastable phases. It has been noted that in real casting conditions Zn-Al alloys have the typical dendrite structure. The consequences of the dendrite structure primarily result in lower ductility, as well as relatively high heterogeneity of mechanical properties of the cast alloy [7]. Recently, it has been found that these problems can be overcome to a great extent by introducing additional alloying elements. Silicon Carbide was found to be a very effective alloying element towards improving the mechanical and tribological properties of Al-Zn alloys. It was documented by Varade et. al. in a Zn-Al wear study that the weight percentage of SiC is the wear factor that has the least influence (1.8756%) on dry sliding of Al-Zn alloy metal matrix composites [8].

Due to the abundance of available Zn and its many practical purposes in industrial applications Zn has become the subject of a great deal of research going on today. Since it has been found that Zn can reduce corrosion and oxidation as well as be a main constituent in numerous low wear MMCs, it is expected that Zn-MAX composites may show exciting properties.

APPENDICES

STATUS OF JOURNAL PUBLICATIONS

- [1] “Development of Novel Multifunctional MAX-Al Composites”, S. Gupta, T. Hammann, and R. Johnson (Accepted for publication, Journal of Materials Engineering and Performance - Manuscript ID JMEEP-14-09-7049.R1).
- [2] “Novel Sn Matrix Composites Reinforced with Ti_3SiC_2 (nanolaminates) Particulates”, T. Hammann, R. Johnson, and S. Gupta (to be submitted).
- [3] “Tribological Behavior of Novel Ti_3SiC_2 (Natural Nanolaminates) Reinforced Epoxy Composites during Dry Sliding”, S. Gupta, T. Hammann, and R. Johnson (Accepted for publication, Tribology Transactions - Manuscript UTRB-1581.R1).

CONTRIBUTED PRESENTATIONS

- [1] “Novel MAX (Nanolaminates) -Al (Aluminum) Multifunctional Composites”, T. Hammann*, S. Gupta, R. Johnson, M.F. Riyad, (MS&T, 2014).
- [2] “Novel Methods for Manufacturing Porous Ceramics”, S. Gupta, M.F. Riyad*, T. Hammann, R. Johnson, (MS&T, 2014).
- [3] “On the Development of Novel Light Weight Multifunctional Composites”, S. Gupta, R. Johnson, T. Hammann*, M.F. Riyad, (MS&T, 2014).
- [4] “On the Development of Next Generation Green Manufacturing Technologies”, S. Gupta*, M.F. Riyad, T. Hammann, R. Johnson, (MS&T, 2014).

- [5] “Development of Novel MAX-Al Composites” T. Hammann*, R. Johnson, M.F. Riyad, S. Gupta, University of North Dakota, USA. 2014 Scholarly Forum, University of North Dakota (2014).
- [6] “On the Development of Novel MAX-Al Composites” T. Hammann*, R. Johnson, M.F. Riyad, S. Gupta, University of North Dakota, USA. 36th International Conference and Expo on Advanced Ceramics and Composites (ICACC’14). Daytona Beach, Fl. (2014).
- [7] “Tribology of Novel MAX-Al Composites” R. Johnson*, T. Hammann, M.F. Riyad, S. Gupta, University of North Dakota, USA. ICACC’14 Daytona Beach, Fl.
- [8] “Novel Green Manufacturing Technologies” S. Gupta*, M. F. Riyad, T. Hammann, R. Johnson, University of North Dakota, USA. ICACC’14 Daytona Beach, Fl.
- [9] “Novel Processing Methods for Developing Porous Oxides and Carbide Ceramics” M.F. Riyad*, R. Johnson, T. Hammann, S. Gupta, University of North Dakota, ICACC’14 Daytona Beach, Fl.
- [10] “On the Manufacturing and Tribology of MAX-Al Composites” T. Hammann*, R. Johnson*, M.F. Riyad, S. Gupta, University of North Dakota Engineering Seminar Series. (2013).
- [11] “Novel Low Alkali Activated Fly Ash Cement (LAFAC) based Composites” M.F. Riyad, T. Hammann, R. Johnson and S. Gupta, University of North Dakota, USA. 4th Advances in Cementbased Materials, UIUC, (2013).

- [12] “On the Development of Low Alkali Activated Fly Ash Cement (LAFAC)”
Surojit Gupta, M.F. Riyad, R. Johnson and T. Hammann, University of North
Dakota, USA. UIUC, (2013).

REFERENCES

CHAPTER 1

- [1] M.W. Barsoum and M. Radovic. “Elastic and Mechanical Properties of the MAX Phases”, *Annu. Rev. Mater. Res.* 41, 195-227 (2011).
- [2] M.W. Barsoum, T. El-Raghy, “Synthesis and characterization of a remarkable ceramic: Ti_3SiC_2 ”, *J. Am. Ceram. Soc.* 79, 1953–1956 (1996).
- [3] M.W. Barsoum, The $M_{n+1}AX_n$ phases: a new class of solids; thermodynamically stable nanolaminates, *Prog. Solid State Chem.* 28, 201–281 (2000).
- [4] S. Amini, M.W. Barsoum, T. El-Raghy, Synthesis and mechanical properties of fully dense Ti_2SC , *J. Am. Ceram. Soc.* 90 (12), 3953–3958 (2007).
- [5] M. Radovic, M.W. Barsoum, T. El-Raghy, S.M. Wiederhorn, W.E. Luecke, “Effect of temperature, strain rate and grain size on the mechanical response of Ti_3SiC_2 in Tension”, *Acta Mater.* 50, 1297–1306 (2002).
- [6] T El-Raghy, M.W. Barsoum, A. Zavaliangos, S.R. Kalidindi “Processing and mechanical properties of Ti_3SiC_2 . II. Effect of grain size and deformation temperature”, *J. Am. Ceram. Soc.* 82, 2855–2860 (1999).
- [7] T. Zhen, M.W. Barsoum, S.R. Kalidindi, M. Radovic, Z.M. Sun, T. El-Raghy “Compressive creep of fine and coarse-grained Ti_3SiC_2 in air in the 1100–1300 °C temperature range”, *Acta Mater.* 53, 4963–4973 (2005).

- [8] S.B. Li, L.F. Cheng, L.T. Zhang “Oxidation behavior of Ti_3SiC_2 at high temperature in air”, Mater. Sci. Eng. Struct. Mater. Prop. Microstruct. Process. 341, 112–120 (2003).
- [9] S. Gupta, M.W. Barsoum, “Synthesis and oxidation of V_2AlC and $(Ti_{0.5},V_{0.5})_2AlC$ in air”, J. Electrochem. Soc. 151, D24–D29 (2004).
- [10] M.W. Barsoum, N. Tzenov, A. Procopio, T. El-Raghy, M. Ali, “Oxidation of $Ti_{n+1}AlX_n$ ($n = 1-3$ and $X = C, N$). II. Experimental results”, J. Electrochem. Soc. 148, C551–C562 (2001).
- [11] X.H. Wang, Y.C. Zhou, “Oxidation behavior of Ti_3AlC_2 powders in flowing air”, J. Mater. Chem. 12 (9), 2781–2785 (2002).
- [12] S. Gupta, D. Filimonov, M.W. Barsoum, “Isothermal oxidation of Ta_2AlC in air”, J. Am. Ceram. Soc. 89, 2974–2976 (2006).
- [13] Z.J. Lin, M.S. Li, J.Y. Wang, Y.C. Zhou, “High-temperature oxidation and hot corrosion of Cr_2AlC ”, Acta Mater. 55, 6182–6191 (2007).
- [14] S. Gupta and M.W. Barsoum “On the tribology of the MAX phases and their composites during dry sliding: A review”, , Wear 271, 1878– 1894 (2011).
- [15] Y. Zhang, Z.M. Sun, Y.C. Zhou, “Cu/ Ti_3SiC_2 composite: a new electrofriction material”, Mater. Res. Innov. 3 80–84 (1999).
- [16] S. Gupta, D. Filimonov, T. Palanisamy, T. El-Raghy and M. W. Barsoum, “ Ta_2AlC and Cr_2AlC Ag-based composites - New solid lubricant materials for use over a wide temperature range against Ni-based superalloys and alumina”, Wear 262, 1479-1489 (2007).

- [17] Anasori, S. Amini, V. Presser, and M. W. Barsoum, “Nanocrystalline M-matrix composites with ultrahigh damping properties”, *B. Magnesium Technology 2011*, John Wiley and Sons, Inc, 463-468 (2011).
- [18] W.J. Wang, V. Gauthier-Brunet, G.P. Bei, G. Laplanche, J. Bonneville, A. Joulain, S. Dubois, “Powder metallurgy processing and compressive properties of Ti_3AlC_2/Al composites”, *Mater. Sci. Eng. A* 530, 168–173 (2011).
- [19] L. Hu, A. Kothalkar, M. O’Neil, I. Karaman, M. Radovic, “Current-activated, pressure-assisted infiltration: a novel, versatile route for producing interpenetrating ceramic–metal composites”, *Mater. Res. Lett.* (2014), <http://dx.doi.org/10.1080/21663831.2013.873498>.
- [20] A. Kothalkar, R. Benitez, L. Hu, M. Radovic, I. Karaman, “Thermo-mechanical response and damping behavior of shape memory alloy/MAX phase composites”, *Metall. Mater. Trans. A*. 45, 2646–2658 (2014).
- [21] K. G. Budinski and M. K. Budinski, “Engineering Materials Properties and Selection”, Prentice Hall, 9th Edition (2010).
- [22] D.B. Miracle, “Metal matrix composites – From science to technological significance”, *Composites Science and Technology* 65, 2526–2540 (2005).
- [23] Z Chen, T. Takeda, K. Ikeda, “Microstructural evolution of reactive-sintered aluminum matrix composites”, *Composites Science and Technology* 68 2245–2253 (2008).

- [24] A. Pramanik, L.C. Zhang, J.A. Arsecularatne, “Machining of metal matrix composites: Effect of ceramic particles on residual stress, surface roughness and chip formation”, *International Journal of Machine Tools & Manufacture* 48 1613–1625 (2008).
- [25] M. El-Gallab, M. Sklad, “Machining of Al/SiC particulate metal-matrix composites, Part I: tool performance”, *Journal of Materials Processing Technology*, 83 151–158 (1998).
- [26] X. Ding, W.Y.H. Liew, X.D. Liu “Evaluation of machining performance of MMC with PCBN and PCD tools”, *Wear*, 259 1225–1234 (2005).

CHAPTER II

- [1] Prasad, B. K., Venkateswarlu, K., Modi, O. P. and Yegneswaran, A. H. 1996. “Influence of the Size and Morphology of Silicon Particles on the Physical, Mechanical and Tribological Properties of Some Aluminium–Silicon Alloys,”. *Journal of Materials Science Letters*, 15: 1773–1776.
- [2] Torabian, H. and Pathak, J. P. 1994. “The Effect of Silicon Content and Morphology on the Wear of Al-Si Alloys under Dry and Lubricated Sliding Conditions,”. *Tribology International*, 27(3): 171–176.
- [3] Torabian, H., Pathak, J. P. and Tiwari, S. N. 1994. “On Wear Characteristics of Leaded Aluminium–Silicon Alloys,”. *Wear*, 177(2): 47–54.
- [4] Rajan, T. V. 1995. “Seizure Failure of Cu-Pb with Overlay and Al-Sn Connecting Rod Bearing,”. *Tribology Transactions*, 36(1): 121–124.

- [5] Gayle, F. W. and Vadersande, J. B. 1986. *Proceedings of International Conferences on Aluminium Alloys: Their Physical and Mechanical Properties (ICAA), Vol. 727*, Warley Engineering Materials Advisory Service.
- [6] Pathak, J. P. and Mohan, S. 2003. "Tribological Behaviour of Conventional Al-Sn Equivalent to Al-Pb Alloys under Lubrication,". *Materials Science*, 26(3): 315–320.

CHAPTER III

- [1] "On the tribology of the MAX phases and their composites during dry sliding: A review", S. Gupta and M.W. Barsoum, *Wear* 271, 1878– 1894 (2011).
- [2] "MAX phases as solid lubricant materials", S. Gupta, T. Palanisamy, M.W. Barsoum and C.W. Li, (U.S Patent 7,553,564 BA, June 30, 2009).
- [3] "MAX Phases with additives as solid lubricant materials", T. Palanisamy, S. Gupta, C. W. Li and M. W. Barsoum, (US Patent 7.572,313 B2, Aug. 11, 2009).
- [4] "Tribological behavior of select MAX phases against Al₂O₃ at elevated temperatures", S. Gupta, D. Filimonov, T. Palanisamy and M. W. Barsoum, *Wear* 265, 560-565 (2008).
- [5] S. Gupta, D. Filimonov, V. Zaitsev, T. Palanisamy and M. W. Barsoum, "Ambient and 550°C tribological behavior of select MAX phases against Ni-based superalloys", *Wear* 264, 270-278 (2008).
- [6] S. Gupta, D. Filiminov, T. Palanisamy, T. El-Raghy and Michel. W. Barsoum, "Tribology of Ti₂SC – a novel MAX Phase", *J. Am. Ceram. Soc.* 90, 3566-3571 (2007).

- [7] S. Gupta, D. Filimonov, T. Palanisamy, T. El-Raghy and M. W. Barsoum, “Ta₂AlC and Cr₂AlC Ag-based composites - New solid lubricant materials for use over a wide temperature range against Ni-based superalloys and alumina”, *Wear* 262, 1479-1489 (2007).
- [8] S. Gupta, D. Filimonov, V. Zaitsev, T. Palanisamy, T. El-Raghy, M.W. Barsoum, “Study of tribofilms formed during dry sliding of Ta₂AlC/Ag or Cr₂AlC/Ag composites against Ni-base superalloys and Al₂O₃”, *Wear* 267, 1490-1500 (2009).
- [9] S. Gupta, D. Filimonov, T. Palanisamy, T. El-Raghy and M. W. Barsoum, “Ta₂AlC and Cr₂AlC Ag-based composites - New solid lubricant materials for use over a wide temperature range against Ni-based superalloys and alumina”, *Wear* 262, 1479-1489 (2007).
- [10] S. Gupta, D. Filimonov, V. Zaitsev, T. Palanisamy, T. El-Raghy, M.W. Barsoum, “Study of tribofilms formed during dry sliding of Ta₂AlC/Ag or Cr₂AlC/Ag composites against Ni-base superalloys and Al₂O₃”, *Wear* **267**, 1490-1500 (2009).
- [11] A.A. Voevodin, “Chameleon coatings: Adaptive surfaces to reduce friction and wear in extreme environments C. Muratore”, *Annu. Rev. Mater. Res.* **39** 297–324 (2009).
- [12] S. Amini, C. Ni, M. W. Barsoum, “Processing, microstructural characterization and mechanical properties of a Ti₂AlC/nanocrystalline Mg-matrix composite”, *Comp. Sci. and Tech.* **69**, 414–420 (2009).
- [13] B. Anasori, S. Amini, V. Presser, and M. W. Barsoum, “Nanocrystalline M-matrix composites with ultrahigh damping properties”, *Magnesium Technology 2011*, John Wiley and Sons, Inc, 463-468 (2011).

- [14] S. Amini, M. W. Barsoum, “On the effect of texture on the mechanical and damping properties of nanocrystalline Mg-matrix composites reinforced with MAX phases”, *Mat. Sci.& Eng. A* **527**, 3707-3718 (2010).
- [15] P. Hasim, T. Nihat, “Investigation of the wear behaviour of a glass–fiber reinforced composite and plain polyester resin”, *Compos Sci Technol* **62**, 367–70 (2002).
- [16] N. Mohan, S. Natarajan, S.P. Kumaresh Babu, “Abrasive wear behaviour of hard powders filled glass fabric–epoxy hybrid composites”, *Materials and Design* **32**, 1704–1709 (2011).
- [17] L. Chang, Z. Zhang, C. B. K. Friedrich, “Tribological properties of epoxy nanocomposites I. Enhancement of the wear resistance by nano-TiO₂ particles”, *Wear* **258**, 141–148 (2005).
- [18] L. Changa, Z. Zhang, L. Ye, K. Friedrich, “Tribological properties of epoxy nanocomposites III. Characteristics of transfer films”, *Wear* **262**, 699–706 (2007).
- [19] S. Basavarajappa, S. Ellangovan, “Dry sliding wear characteristics of glass–epoxy composite filled with silicon carbide and graphite particles”, *Wear* **296**, 491–496 (2012).
- [20] L. Chang, K. Friedrich, “Enhancement effect of nanoparticles on the sliding wear of short fiber-reinforced polymer composites: A critical discussion of wear mechanisms”, *Tribology International* **43**, 2355–2364 (2010).
- [21] C. Min, D. Yu, J. Cao, G. Wang, L. Feng, “A graphite nanoplatelet/epoxy composite with high dielectric constant and high thermal conductivity”, *Carbon* **55**, 116–125 (2013).

- [22] Z. Jia, Y. Yanga, “Self-lubricating properties of PTFE/serpentine nanocomposite against steel at different loads and sliding velocities”, *Composites: Part B* **43**, 2072–2078 (2012).
- [23] Q. B. Guoa, M. Z. Rong, G. Liang Jia, K. T. Lau, M. Q. Zhang, “Sliding wear performance of nano-SiO₂/short carbon fiber/epoxy hybrid composites”, *Wear* **266**, 658–665 (2009).
- [24] S. Gupta and M.W. Barsoum “On the tribology of the MAX phases and their composites during dry sliding: A review”, *Wear* **271**, 1878– 1894 (2011).
- [25] S. Gupta, “Tribology of MAX phases and their composites”, PhD Thesis, Drexel University (2006).
- [26] M.W. Barsoum, T. El-Raghy, “Synthesis and characterization of a remarkable ceramic: Ti₃SiC₂”, *J. Am. Ceram. Soc.* **79**, 1953–1956 (1996).
- [27] T. El-Raghy, P. Blau, M.W. Barsoum, Effect of grain size on friction and wear behavior of Ti₃SiC₂, *Wear* **238** (2) (2000) 125–130.
- [28] A. Souchet, J. Fontaine, M. Belin, T. Le Mogne, J.-L. Loubet, M.W. Barsoum, “Tribological duality of Ti₃SiC₂”, *Tribol. Lett.* **18**, 341–352 (2005).

CHAPTER IV

- [1] “Public Health Statement Zinc”, ATSDR CAS#7440-66-6 (2005).
- [2] “Microstructures of Various Zinc Coatings”, American Galvanizers Association, (2006).
- [3] S.C. Sharma, B.M. Satish, B.M. Girish, R. Kamath, H. Asanuma, “Dry Sliding Wear of Short Glass Fibre Reinforced Zinc-Aluminum Composites”, Tribology International. Vol. 31, Issue 4, 183-188 (1998).
- [4] A.T. Alpas, J. Zhang, “Effect of SiC Particulate Reinforcement on the Dry Sliding Wear of Al-Si Alloys”, Wear, Res. 155, 83-104 (1996).
- [5] B.K. Prasad, “Effectiveness of an Externally Added Solid Lubricant on the Sliding Wear Response of a Zn-Al alloy, its Composite and Cast Iron”, Tribology Letters. Vol. 18, No. 2, 135-143 (2005).
- [6] B.K. Prasad, “Abrasive Wear Characteristics of a Zn-Based Alloy and Zn-alloy/SiC Composite”, Wear. Vol. 252, Issue 3-4, 250-263 (2002).
- [7] Z. Azakh, T. Savas-Kan, “An Examination of Friction and Sliding wear Properties of Zn—40Al-2Cu-2Si Alloy in case of Oil Cut Off”, Tribology International, Vol. 42 176-182 (2008).
- [8] H.P. Varade, A.G. Thakur, P.M. Patare, N.D. Sadaphal, “Wear Studies of Al-Zn Alloy Metal Matrix Composites”, Int. Journal of Eng. Sci. and Tech. Vol. 5, No. 5 978-983 (2013).